

Reaction of Sc⁺, Ti⁺, and V⁺ with CO. MC⁺ and MO⁺ bond energies

D. E. Clemmer, J. L. Elkind,^{a)} N. Aristov,^{b)} and P. B. Armentrout^{c)}
Department of Chemistry, University of Utah, Salt Lake City, Utah 84112

(Received 16 April 1991; accepted 28 May 1991)

The reactions of Sc⁺, Ti⁺, and V⁺ with CO are studied as a function of translational energy in a guided-ion-beam tandem mass spectrometer. Formation of both metal-carbide and metal-oxide ions are observed and rationalized by a direct atom abstraction mechanism. At high energies, the ScC⁺ and ScO⁺ cross sections exhibit additional features that are unusual but can be explained by an impulsive pairwise mechanism and formation of excited-state product ions, respectively. Thresholds of the reaction cross sections are interpreted to give the 0 K bond energies (in eV) $D^0(\text{ScC}^+) = 3.34 \pm 0.06$, $D^0(\text{TiC}^+) = 4.05 \pm 0.24$, $D^0(\text{VC}^+) = 3.87 \pm 0.14$, $D^0(\text{ScO}^+) = 7.11 \pm 0.08$, $D^0(\text{TiO}^+) = 6.88 \pm 0.07$, and $D^0(\text{VO}^+) = 5.81 \pm 0.17$. Additional studies are used to help verify the bond energy for ScO⁺ and yield a recommended value of 7.14 ± 0.11 eV. The nature of the bonding in MO⁺ and MC⁺ is discussed and compared for these three metal ions.

I. INTRODUCTION

Recently, we reported a comprehensive set of experimental bond energies for the first-row diatomic transition-metal-oxide ions.¹ The most reliable bond energies for ScO⁺, TiO⁺, and VO⁺ came from literature values of the ionization energies (IE) and bond energies of the neutral MO molecule, listed in Table I, as calculated by Eq. (1):

$$D^0(\text{MO}^+) = D^0(\text{MO}) - \text{IE}(\text{MO}) + \text{IE}(\text{M}). \quad (1)$$

While values for TiO⁺ and VO⁺ are quite precise, the bond energy for ScO⁺, 6.9 ± 0.3 eV, has a broad error range due to the uncertainty associated with IE(ScO).² In the present study, we use guided-ion-beam mass spectrometry to directly measure complementary and independent ionic metal-oxide thermochemistry from the reactions of Sc⁺, Ti⁺, and V⁺ with carbon monoxide. Only in the case of VO⁺ have such direct measurements of the metal-oxide bond energy been made previously.^{3,4} These reaction systems also provide bond energies for the ionic metal carbides, species for which thermochemistry is scarce. The thermochemistry of such metal-carbide and -oxide species is of interest due to its importance to organometallic and atmospheric⁵ chemistry, and in understanding corrosion processes.²

Aristov and Armentrout (AA) previously reported preliminary thermochemical results measured from the V⁺ + CO system.³ They cited values of $D^0(\text{VO}^+) = 5.68 \pm 0.22$ eV and $D^0(\text{VC}^+) = 3.82 \pm 0.22$ eV. The former value is somewhat lower than both $D^0(\text{VO}^+) = 6.00 \pm 0.35$ eV determined by collision-induced dissociation,⁴ and the most precise value, $D^0(\text{VO}^+) = 5.99 \pm 0.10$, obtained by using Eq. (1).¹ The bond energy for VC⁺ agrees with a more precise value, $D^0(\text{VC}^+) = 3.95 \pm 0.04$ eV, determined from the reactions of V⁺ with ethane, ethene, and ethyne.⁶ In the present

study, we derive thermochemistry from the results for the V⁺ + CO system by using a more comprehensive analysis that includes the reactivity due to excited states in the beam. Further, we extend the study to titanium and scandium in order to verify the MO⁺ thermochemistry, determine trends in MC⁺ bonding, and understand the mechanism that leads to breaking the very strong CO bond, $D_0^0(\text{CO}) = 11.108 \pm 0.005$ eV.⁷

II. EXPERIMENT

A. General

Complete descriptions of the apparatus and experimental procedures are given elsewhere.⁸ Sc⁺, Ti⁺, and V⁺ production is described below. The ions are extracted from the source, accelerated, and focused into a magnetic sector momentum analyzer for mass analysis. Mass-selected ions are slowed to a desired kinetic energy and focused into an octopole ion guide which radially traps the ions. The octopole passes through a static gas cell containing the neutral reactant. Neutral gas pressures in the cell are kept low (~ 0.1 to 0.2 mTorr) so that multiple ion-molecule collisions are improbable. After exiting the gas cell, product and unreacted beam ions drift to the end of the octopole where they are directed into a quadrupole mass filter for mass analysis and then detected. Ion intensities are converted to absolute cross sections as described previously.⁸ Uncertainties in cross sections are estimated to be $\pm 20\%$.

Laboratory ion energies relate to center-of-mass (CM) frame energies by $E_{\text{CM}} = E_{\text{lab}} m / (M + m)$, where M and m are the ion and neutral reactant masses, respectively. Absolute energy scale uncertainties are ± 0.05 eV lab. The data obtained in these experiments are broadened by two effects: the spread in the ion energy, which is independent of energy, and thermal motion of the neutral gas, which has a width of $\sim 0.46E_{\text{CM}}^{1/2}$ for these reactions.⁹ The zero of the absolute energy scale and the ion energy distribution (full width at half maximum of ≈ 0.7 eV, lab) are measured by a retarding potential technique described in detail elsewhere.⁸

^{a)} Present address: Texas Instruments, Dallas, TX 75265.

^{b)} Present address: Springer-Verlag, 6900 Heidelberg 1, Federal Republic of Germany.

^{c)} Camille and Henry Dreyfus Teacher-Scholar, 1987-1992.

TABLE I. Thermochemistry for diatomic metal carbides and oxides (eV) at 0 K.

| ML ⁺ | IE(M) ^a | $D_0^\circ(\text{ML}^+)^b$ | $\Delta_f H_0(\text{ML}^+)^c$ | IE(ML) ^b | $D_0^\circ(\text{ML})$ |
|------------------|--------------------|----------------------------|-------------------------------|---------------------------|--------------------------|
| ScO ⁺ | 6.562 | 6.9(0.3) ^d | 6.2(0.3) | 6.6(0.3) ^e | 7.01(0.12) ^f |
| | | 7.11(0.08) | 5.99(0.11) | | |
| | | 7.14(0.11) ^g | 5.96(0.14) | 6.43(0.16) ^d | |
| TiO ⁺ | 6.820(0.006) | 6.93(0.10) ^d | 7.42(0.12) | 6.819(0.006) ^h | 6.92(0.10) ^f |
| | | 6.88(0.07) | 7.47(0.10) | | |
| VO ⁺ | 6.740(0.002) | 5.99(0.10) ^d | 8.72(0.13) | 7.230(0.005) ⁱ | 6.48(0.09) ^j |
| | | 5.81(0.17) | 8.90(0.19) | | |
| ScC ⁺ | 6.562 | 3.34(0.06) | 14.57(0.10) | >5.11 ^d | <4.56(0.22) ^k |
| TiC ⁺ | 6.820(0.006) | 4.05(0.24) | 15.12(0.25) | | |
| VC ⁺ | 6.740(0.002) | 3.87(0.14) | 15.65(0.16) | | |
| | | 3.95(0.04) ^l | 15.57(0.09) | | |

^a Values are from Ref. 11.

^b Unless otherwise stated, the tabulated thermochemistry is from this study.

^c Ion heats of formation are calculated using the thermal electron convention. $\Delta_f H^0(\text{Sc}^+) = 10.54 \pm 0.08$ eV from Wagman *et al.*, *J. Phys. Chem. Ref. Data* **11**, Suppl. 2, (1982); $\Delta_f H^0(\text{Ti}^+) = 11.797 \pm 0.065$ eV from Ref. 7, and $\Delta_f H^0(\text{V}^+) = 12.15 \pm 0.08$ eV from Ref. 7.

^d Derived by using Eq. (1).

^e Reference 2.

^f Reference 27.

^g Average value derived from reactions (4), (6), and (7) as discussed in the text.

^h A. D. Sappey, G. Eiden, J. E. Harrington, and J. C. Weisshaar, *J. Chem. Phys.* **90**, 1415 (1989).

ⁱ J. Harrington and J. C. Weisshaar (personal communication). This value is consistent with 7.25 ± 0.01 eV taken from J. M. Dyke, B. W. J. Gravenor, M. P. Hastings, and A. Morris, *J. Phys. Chem.* **89**, 4613 (1985).

^j G. Balducci, G. Gigli, and M. Guido, *J. Chem. Phys.* **79**, 5616 (1983).

^k Reference 28.

^l Reference 6.

B. Ion sources

Sc⁺, Ti⁺, and V⁺ are produced by surface ionization (SI). In the SI source, the metal is introduced to the gas phase as TiCl₄ (Aldrich 99.9%) or VOCl₃ (Alfa 99.995%) vapor or by vaporizing ScCl₃ · 6H₂O (Aesar) in an oven. The metal-containing vapor is directed toward a resistively heated rhenium filament where it decomposes and the resulting metal atoms are ionized. It is generally assumed that ions produced by SI equilibrate at the temperature of the filament and the state populations are governed by a Maxwell-Boltzmann distribution. The validity of this assumption has been discussed previously.¹⁰ The temperature of the SI filament used to produce ions in these experiments is 2225 ± 200 K for Sc⁺, and 1950 ± 200 K for Ti⁺ and V⁺. Under these conditions, the beams comprise mostly ground-state ions; 88% Sc⁺ (*a*³D) ground state with Sc⁺ (*a*¹D) first and Sc⁺ (*a*³F) second excited states each making up 6% of the beam; 65% Ti⁺ (*a*⁴F) ground state with 34% Ti⁺ (*b*⁴F) first excited state also present; 84% V⁺ (*a*⁵D) with 16% V⁺ (*a*³F) also present. Exact populations and energies¹¹ of the low-lying states populated in these SI beams have been tabulated previously.^{12,13}

C. Thermochemical analyses

Theory^{14,15} and experiment¹⁶⁻¹⁸ indicate that cross sections for endothermic reactions can be modeled by

$$\sigma(E) = \sum_i g_i \sigma_0 (E - E_0 + E_i + E_{\text{int}})^n / E, \quad (2)$$

which involves an explicit sum of the contributions of individual states, denoted by *i*, weighted by their populations, *g_i*. Here, σ_0 is a scaling factor, *E* is the relative kinetic energy, *n* is an adjustable parameter, *E₀* is the threshold for reaction of the lowest electronic level of the ion [Sc⁺ (*a*³D₁), Ti⁺ (*a*⁴F_{3/2}), and V⁺ (*a*⁵D₀)], and *E_i* is the electronic excitation of each particular electronic state (for convenience, we use *J*-averaged values). *E_{int}* is the internal energy of the neutral reagent, which for room-temperature CO is only the rotational energy, 0.026 eV. Thus, *E₀* is the threshold for reaction at 0 K. The σ_0 , *n*, and *E₀* parameters are optimized by using a nonlinear least-squares analysis to give the best fit to the data after convoluting over the neutral and ion kinetic-energy distributions as described previously.⁸ Error limits for *E₀* are calculated from the range of threshold values obtained for different data sets with different values of *n* and the error in the absolute energy scale.

III. RESULTS

The reactions of M⁺ (M = Sc, Ti, and V) with CO yield two ionic products, corresponding to reactions (3) and (4). The cross sections for these



reactions when Sc⁺, Ti⁺, and V⁺ are produced by SI are displayed in Figs. 1–3. All three systems have MC⁺ and MO⁺ cross sections that peak near the CO bond energy of 11.11 eV. This implies that the cross sections decline at higher energies due to reaction (5):



At all energies, the cross sections for MO⁺ formation are larger than those for MC⁺ production (factors of ~ 3.5 for M = Sc, and ~ 4.0 for M = Ti and V, respectively, at the 11 eV peaks). The observation that $\sigma(\text{MO}^+) > \sigma(\text{MC}^+)$ is consistent with the thermodynamics associated with reactions (3) and (4), as evidenced by the higher threshold for formation of MC⁺ than for MO⁺.

Compared to the results for Ti⁺ and V⁺, the cross sections for ScC⁺ and ScO⁺ are more complex. $\sigma(\text{ScC}^+)$ exhibits a second feature that peaks at ~ 17 eV. This second peak has roughly the same magnitude as the lower-energy peak ($\sim 0.10 \text{ \AA}^2$). $\sigma(\text{ScO}^+)$ shows a noticeable break in slope between 7 and 8 eV. While such breaks could exist for the TiO⁺ and VO⁺ cross sections, they are not obvious, if present at all.

We have analyzed the cross sections for reactions (3) and (4) for M = Sc, Ti, and V with Eq. (2). All electronic states present in the ion beam are included in this analysis and assumed to have equal reaction probabilities. The resulting values of E_0 and the parameters σ_0 and n are given in Table II. All fits for the titanium and vanadium systems and $\sigma(\text{ScC}^+)$ in the scandium system accurately reproduce the data from well below the threshold to near the 11 eV peak of the cross section, the energy where reaction (5) can begin. This is illustrated in Fig. 4 for the titanium system. Thus the multistate analysis of the threshold region appears to ac-

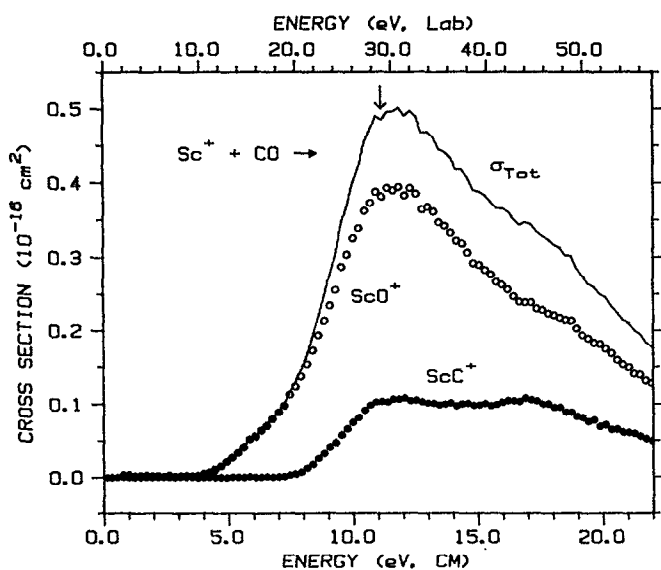


FIG. 1. Variation of product cross sections for reaction of CO with Sc⁺ produced by SI as a function of translational energy in the center-of-mass frame (lower scale) and the laboratory frame (upper scale). Results are shown for ScO⁺ (open circles) and ScC⁺ (solid circles). The solid line represents the total reaction cross section. The arrow at 11.11 eV shows the bond energy $D^0(\text{CO})$.

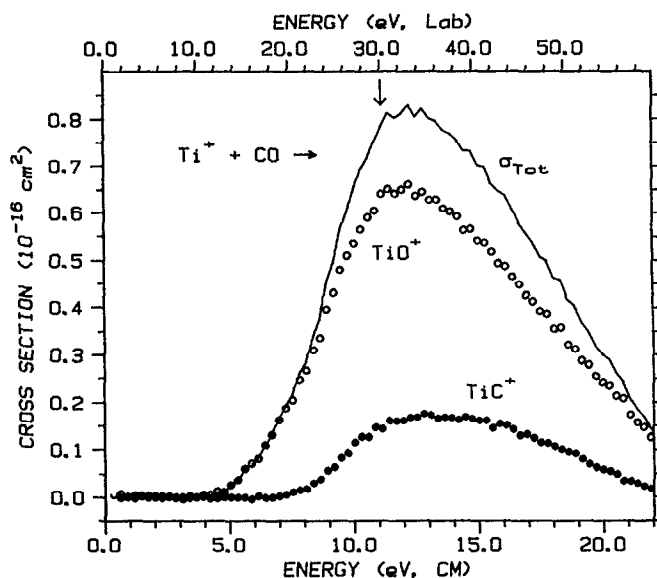


FIG. 2. Variation of product cross sections for reaction of CO with Ti⁺ produced by SI as a function of translational energy in the center-of-mass frame (lower scale) and the laboratory frame (upper scale). Results are shown for TiO⁺ (open circles) and TiC⁺ (solid circles). The solid line represents the total reaction cross section. The arrow at 11.11 eV shows the bond energy $D^0(\text{CO})$.

count for contributions to the cross sections from all electronic states present in the beam.

For $\sigma(\text{ScO}^+)$, Eq. (2) is unable to accurately model the data over a comparably wide energy range. We can reproduce the data either above or below the break in $\sigma(\text{ScO}^+)$ observed between 7 and 8 eV. One possibility for the inability of Eq. (2) to accurately model the data is that

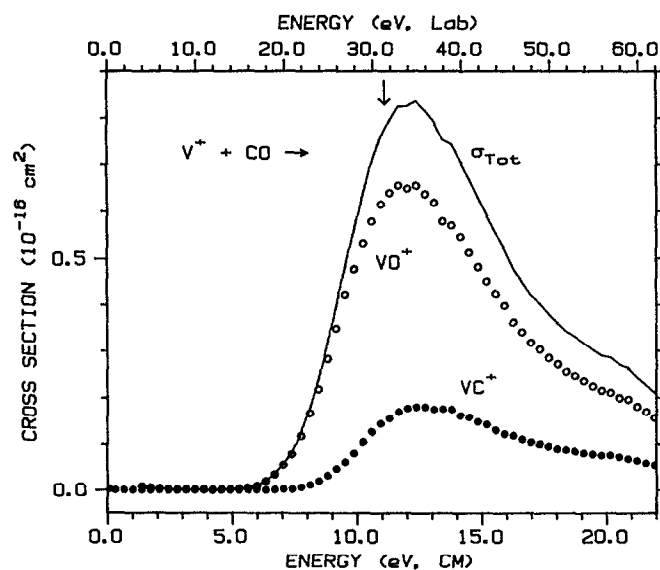


FIG. 3. Variation of product cross sections for reaction of CO with V⁺ produced by SI as a function of translational energy in the center-of-mass frame (lower scale) and the laboratory frame (upper scale). Results are shown for VO⁺ (open circles) and VC⁺ (solid circles). The solid line represents the total reaction cross section. The arrow at 11.11 eV shows the bond energy $D^0(\text{CO})$.

TABLE II. Summary of parameters of Eq. (2) used to fit cross sections.^a

| Product ion | E_0 (eV) | σ_0 | n |
|------------------|------------|------------|----------|
| ScO ⁺ | 4.00(0.08) | 0.08(0.01) | 1.8(0.1) |
| TiO ⁺ | 4.23(0.07) | 0.11(0.02) | 2.2(0.2) |
| VO ⁺ | 5.30(0.17) | 0.05(0.02) | 3.1(0.2) |
| ScC ⁺ | 7.77(0.06) | 0.22(0.02) | 1.5(0.1) |
| TiC ⁺ | 7.05(0.24) | 0.11(0.05) | 2.2(0.4) |
| VC ⁺ | 7.24(0.14) | 0.06(0.02) | 2.5(0.3) |

^aUncertainties are in parentheses.

the reactivities of the various electronic states present in the beam differ. We have previously observed this type of behavior for reactions of low-spin and high-spin states of Ti⁺ and V⁺ with other molecules.^{6,10,12,13,19,20} To test this hypothesis, we attempted to model the data by enhancing the reactivity of excited states relative to the ground state. Two variations were considered. First, the data were modeled by allowing the reactivity of the low-lying ¹D states (both individually and together) to be greater than that for the triplet states by factors up to 100. Second, we considered the possibility that reactive differences were due to differences in electron configuration by allowing states with a 3d² configuration (the *a*³F and *b*¹D states) to react more efficiently (again by factors up to 100) than states with a 4s3d configuration (the *a*³D and *a*¹D states). In neither case were any major improvements in representing the data over the entire energy range achieved.

Another possible explanation for the break observed in

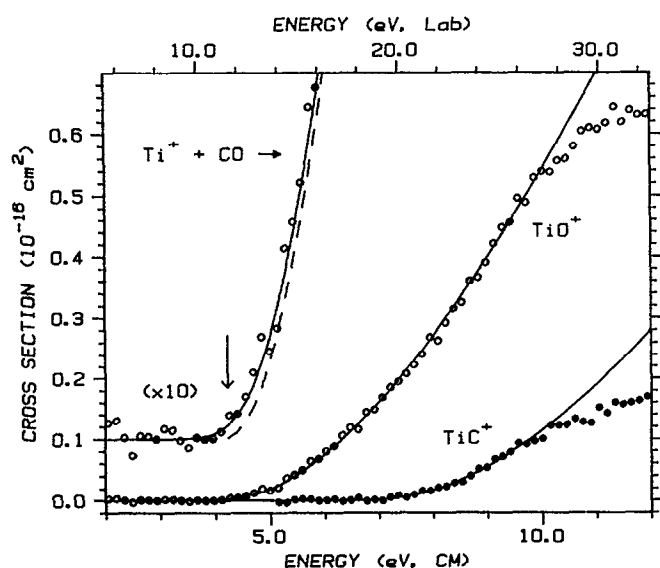


FIG. 4. Cross sections in the threshold region for formation of TiO⁺ (open circles) and TiC⁺ (solid circles) in the reaction of Ti⁺ with CO as a function of kinetic energy in the center-of-mass frame (lower scale) and laboratory frame (upper scale). The inset shows the TiO⁺ data expanded by a factor of 10 and offset from zero. The solid lines are from Eq. (2) with the parameters in Table II convoluted over the experimental energy distribution, while the dashed line shows the unconvoluted model. The arrow at 4.23 eV shows the threshold for reaction (4).

$\sigma(\text{ScO}^+)$ is that an additional process begins near this energy. Assuming this hypothesis to be true, we have analyzed the threshold region of $\sigma(\text{ScO}^+)$ with Eq. (2) by fitting the data only up to ~ 7.0 eV. The results of this analysis lead to similar parameters as were found for $\sigma(\text{TiO}^+)$ and are given in Table II.

Although the analysis becomes more speculative, further progress in understanding the anomalous cross-section shapes for Sc⁺ in processes (3) and (4) can be made. As shown in Fig. 5, both the ScC⁺ and the ScO⁺ cross sections can be reproduced by assuming that two processes are occurring. The low-energy portions of both cross sections are accurately modeled by Eq. (2) using the parameters given in Table II. At higher energies, these model cross sections are modified to account for the decline of the cross section due to dissociation of the product ion, reaction (5). This is achieved by using a statistical model that conserves angular momentum and has been discussed in detail previously.²¹ For both reactions, the threshold for product dissociation is set to $D^0(\text{CO}) = 11.11$ eV. To account for the remainder of the experimentally observed cross sections, model cross sections for a high-energy process were obtained by subtracting the low-energy models from the experimental cross sections, and fitting the remaining data with Eq. (2), including the dissociation model. Both high-energy models have optimum fits that have a line-of-centers form, Eq. (2) with $n = m = 1$. For ScO⁺, the high-energy process begins at ~ 8.0 eV and dissociates at $D^0(\text{CO})$, while for ScC⁺, the high-energy reactivity begins at ~ 12.5 eV, and falls off at ~ 17.5 eV. Figure 5 shows that the sum of the low- and high-energy models reproduces the experimental cross sections very well from threshold to about 19 eV.

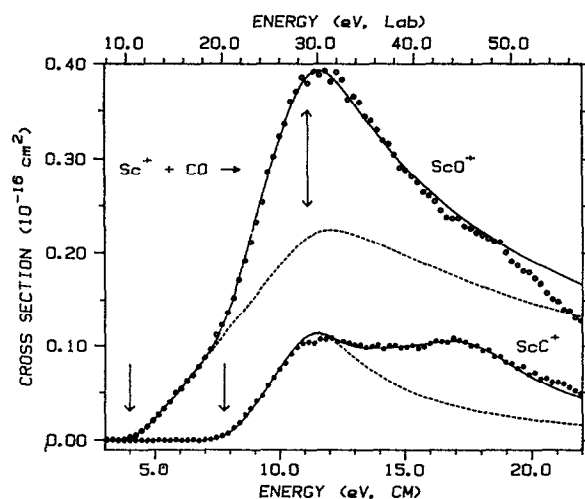


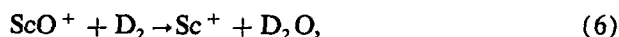
FIG. 5. Cross sections for formation of ScO⁺ (open circles) and ScC⁺ (solid circles) in the reaction of Sc⁺ with CO as a function of kinetic energy in the center-of-mass frame (lower scale) and laboratory frame (upper scale). The dashed lines show the low-energy model cross sections given by Eq. (2) and the parameters given in Table II convoluted over the experimental energy distribution. The solid lines are the sums of these models and models for higher-energy processes (discussed in text). The arrows at 4.00, 7.77, and 11.11 eV show the thresholds for reactions (4), (3), and (5), respectively.

IV. DISCUSSION

A. Thermochemistry

By assuming that E_0 is the enthalpy difference between reactants and products, we can calculate the metal–ligand bond energies of the products at 0 K. This implies that there are no activation barriers in excess of the endothermicity, an assumption that is often true for ion–molecule reactions.^{22,23} Combining the thresholds in Table II with $D_0^0(\text{CO}) = 11.11$ eV gives the 0 K MC⁺ and MO⁺ bond energies listed in Table I. It can be seen that the value for TiO⁺ is in excellent agreement with the literature data. For VO⁺, we obtain a value that is within experimental error of the best literature thermochemistry and AA's preliminary value, 5.68 ± 0.22 eV.³ The present value differs somewhat from the preliminary result primarily because the shape of the reaction cross section in the threshold region has been more accurately represented using the multistate model of Eq. (2).

The bond energy for ScO⁺ determined here, $D^0(\text{ScO}^+) = 7.11 \pm 0.08$ eV, is slightly higher and more precise than the literature value, Table I, although they agree within the rather large uncertainty in the latter value. We have further tested the accuracy of our ScO⁺ bond energy by measuring the thresholds for reactions (6) and (7).^{24,25} Combining these thresholds with



the appropriate thermochemistry gives $D_0^0(\text{ScO}^+) = 7.15 \pm 0.10$ and 7.16 ± 0.15 eV, respectively,^{26,27} in excellent agreement with the bond energy determined here. Our best value for the ScO⁺ bond energy is an average of the thermochemistry for these three systems, $D_0^0(\text{ScO}^+) = 7.14 \pm 0.11$ (Table I). This value can be used to calculate a more precise value for the ionization energy of ScO by use of Eq. (1), $\text{IE}(\text{ScO}) = 6.43 \pm 0.16$ eV, in agreement with the directly measured value.

While there is no reported thermochemistry for ScC⁺ and TiC⁺ that can be compared to our present results, the bond energy derived here for VC⁺ agrees with the value derived from the reactions of V⁺ with C₂ hydrocarbons.⁶ In general, the agreement of the thermochemistry obtained here with previous work ensures that the thresholds determined for reactions (3) and (4) represent the true thermodynamic limit.

Of the carbides, neutral thermochemistry is available only for ScC. Haque and Gingerich have used Knudsen effusion mass spectrometry to determine that $D^0(\text{ScC}) < 4.56 \pm 0.22$ eV.²⁸ This value is much higher than a 1.63 eV lower bound calculated for the ground-state ScC(⁴Π) by Jeung and Koustecky.²⁹ Combining the upper limit for the ScC bond energy with our thermochemistry in an equation analogous to Eq. (1), we obtain a lower limit for the ionization energy of scandium carbide, $\text{IE}(\text{ScC}) > 5.11$ eV.

B. MO⁺ and MC⁺ bonding

We have previously discussed periodic trends in the bonding of the neutral and ionic metal oxides.¹ The high bond energies of ScO⁺, TiO⁺, and VO⁺ have been rationalized as two covalent M–O bonds (since oxygen has two unpaired electrons) enhanced by donation of electron density from the lone pair of 2*p* electrons on the oxygen atom into an empty metal *d* orbital (a dative bond).¹ The net result is that these three early metal-oxide ions have bond energies that are equivalent to triple bonds. The MO⁺ bond energies decrease from ScO⁺ to TiO⁺ to VO⁺ because more *d-d* exchange energy is lost upon bonding as the number of metal *d* electrons increases. Of the early first-row transition metals, this bonding scheme has been confirmed theoretically for ScO⁺,³⁰ VO⁺,³¹ and CrO⁺.^{32,33}

In considering the bonding between a transition metal and a carbon atom, we might expect similarities with the metal–oxide bonding since both atomic carbon and oxygen have ³*P* ground states with two unpaired 2*p* valence electrons. Differences clearly exist, however, since $D^0(\text{MO}^+)$ is larger than $D^0(\text{MC}^+)$ for M = Sc, Ti, and V by 3.8, 2.9, and 2.1 eV, respectively, and $D^0(\text{TiC}^+) > D^0(\text{ScC}^+)$, while for the metal oxides, $D^0(\text{ScO}^+) > D^0(\text{TiO}^+)$. In analogy with our discussion on the bonding of oxygen atoms to metal ions and with calculations of Harrison on CrC⁺,³² we expect that the ground states of the metal-carbide ions result from interaction of the ground-state metal ion and ground-state C(³*P*, 2*s*²2*p*²). For all three metal-carbide ions, two covalent bonds can be formed (either two π bonds or a σ and π bond). This suggests that ScC⁺, TiC⁺ and VC⁺ should have singlet, doublet and triplet spin ground states, respectively. Unlike oxygen, carbon has no lone pair of 2*p* electrons to form a third metal–ligand bond, thus accounting for the relative weakness of $D^0(\text{MC}^+)$ compared to $D^0(\text{MO}^+)$. In the cases of Ti⁺ and V⁺, however, the bonding may be enhanced by donation of nonbonding 3*d* electrons into the empty *p* orbital on the carbon atom (either a σ or a π orbital). (While V⁺ has two valence electrons that could form a two-electron dative bond, this state of VC⁺ correlates with a highly excited state of the V⁺ atom and is probably not important.) If such a backbonding interaction is strong, then the overall bond order for TiC⁺ and VC⁺ is approximately 2(1/2), while that for ScC⁺ is only 2, explaining why TiC⁺ and VC⁺ have stronger bond energies than ScC⁺. As for the metal-oxide ions, $D^0(\text{TiC}^+)$ is greater than $D^0(\text{VC}^+)$ due to differences in *d-d* exchange energies. It is also possible that some *sp* hybridization on the carbon atom occurs, as observed by Harrison in his calculations of CrC⁺,³² and this could change the bonding character somewhat. Calculations on these metal-carbide ions would be useful in addressing the details of the MC⁺ bonds.

C. Mechanism

In previous work involving the reactions of Sc⁺, Ti⁺, and V⁺ with hydrogen,^{34–36} small hydrocarbons,^{6,10,16} and ammonia,^{12,13} the observed reactivity was explained by in-

voking a mechanism that involves oxidative addition of a neutral bond to the metal center. This mechanism is clearly unlikely for the systems studied here since the CO bond energy is so large, 11.11 eV. Further, an O–M⁺–C intermediate cannot have very strong bonds since there are too few metal valence electrons to support the kind of bonding discussed above for *both* ligands. Indeed, any reasonable estimates of the energy of this intermediate place it sufficiently high in energy that it would have little effect upon the dynamics of the reaction.

A more likely mechanism that explains the products of the M⁺ + CO interaction is direct abstraction of either C or O from the CO molecule. Since there is no common intermediate for this mechanism, there is no reason why the MC⁺ and MO⁺ cross sections should appear coupled (in agreement with our experimental observations). We can envision this direct reaction occurring via a linear approach (although the abstractions need not be limited to this geometry). An M⁺ having an electron configuration where the 4s (and to a lesser degree, the 3dσ) orbital is empty can accept electron density from the nonbonding σ electrons on either the O atom or the C atom into the 4s (or 3dσ) orbital thus forming an incipient M–L bond. In addition, occupied 3dπ metal orbitals can simultaneously donate electron density into the antibonding π* molecular orbitals of CO. In this manner, a bond is made between the metal and the ligand, while the CO bond is weakened. Since the nonbonding σ and antibonding π* molecular orbitals of CO are oriented along the ends and away from the CO bond, overlap with the 4s and 3dπ orbitals of M⁺ is maximized for linear geometries and minimized when the M⁺ approach is perpendicular to the CO bond (the approach necessary for M⁺ to insert). Thus, from a molecular-orbital standpoint, it seems likely that a near linear configuration leading to atom abstraction is the most favorable mechanism for reaction.

While this picture of transition-metal–carbonyl bonding is fairly standard, calculations of transition-metal monocarbonyl cations by Bauschlicher and Barnes³⁷ and by Harrison and co-workers³⁸ find that the M⁺–CO bonds are very long and primarily electrostatic. Theoretical results find less than 10% σ donation from the CO ligand to the metal and almost no π donation from the metal to the ligand. While this seems disparate from the picture described above, it should be remembered that the calculations are concerned with the minimum on the MCO⁺ potential-energy surface rather than the interactions necessary to induce reactions (3) and (4). We envision that the elevated kinetic energies necessary for these reactions bring the metal ion and the CO in much closer contact than is found for the equilibrium position. At such distances, it seems likely that the σ donation and π backbonding interactions discussed above become important.

D. High-energy reactivity in the Sc⁺ system

Based on the thermochemistry discussed above, the low-energy cross-section models for reactions (3) and (4) with Sc⁺ appear to represent the true thermodynamic behavior of the system. At higher energies, there appear to be

additional contributions to the scandium cross sections that are not observed in the Ti⁺ and V⁺ systems. While the detailed modeling of these high-energy contributions shown in Fig. 5 is speculative, it is intriguing to consider qualitative explanations for these features. One possibility is that excited-state products are formed. Indeed, Tilson and Harrison³⁰ calculate that there are two triplet ScO⁺ states, ³Δ and ³Σ⁺, lying 3.45 and 4.31 eV, respectively, above the ¹Σ⁺ ground state. These excitation energies are consistent with the position of the slope change observed in σ(ScO⁺) and also with the 4.0 eV difference between the low- (thermodynamic) and high-energy thresholds in Fig. 5. The formation of such excited states may be prominent in the Sc⁺ system because the production of ground-state ScO⁺ (¹Σ⁺) + C(³P) from the Sc⁺ (¹D) excited state, ~6% of the SI-produced beam, is spin forbidden, but formation of the triplet states of ScO⁺ is spin allowed. The singlet states of Sc⁺ are unique in this regard; no states of Ti⁺ or V⁺ nor the triplet states of Sc⁺ have such a similar spin restriction. This explanation for the high-energy feature in the ScO⁺ cross section is also consistent with the observation that the cross section begins to decline near D⁰(CO) (Fig. 5).³⁹

It is possible that the high-energy feature in the ScC⁺ cross section is also due to an excited product state, but this explanation is more complicated in this case since the apparent threshold for such an excited state is *above* D⁰(CO). The only way that this can occur is if the atomic O product is excited or the ScC⁺ product is excited to a state that dissociates only to a high-energy asymptote and not to the ground or low-lying states of Sc⁺ + C. While possible, we have not previously observed such behavior in other reaction systems.

An alternative explanation for the high-energy behavior of the scandium system is that a high-energy impulsive interaction leads to reaction. A model for this process has been described in detail previously,⁴⁰ and assumes that the reaction occurs via impulsive hard-sphere-like interactions between the incoming ion and the first atom it hits. This restricts the amount of the collision energy available for reaction such that the cross sections are shifted up in energy by a constant factor that depends on the masses.⁴¹ For σ(ScC⁺), we find that the reaction and dissociation thresholds for the high-energy feature (12.5 and 17.5 eV, respectively) are both higher than the thermodynamic values (7.8 and 11.1 eV, respectively) by factors of 1.6. This is close to the mass factor predicted by the purely impulsive model, 1.8 for reaction (3). In unpublished work,⁴² we have also seen such a high-energy feature in the reactions of Mn⁺ and Fe⁺ with CO to form MC⁺ (but not MO⁺). The ground states of Mn⁺ and Fe⁺ have high-spin 4s¹3dⁿ configurations that have previously been observed to exhibit this kind of impulsive reactivity with HD.^{40,43} Thus, Sc⁺ may exhibit such behavior due to its ³D(4s¹3d¹) ground state, while the ⁵D(3d⁴) ground state of V⁺ does not exhibit such behavior. While the a⁴F(4s¹3d²) ground state of Ti⁺ might also be expected to exhibit such impulsive behavior, the b⁴F(3d³) state is very close in energy to the a⁴F state such that extensive mixing between these configurations probably occurs during reaction, as suggested previously.^{10,13,35}

ACKNOWLEDGMENT

This work was supported by the National Science Foundation, under Grant No. CHE-8917980.

- ¹ E. R. Fisher, J. L. Elkind, D. E. Clemmer, R. Georgiadis, S. K. Loh, N. Aristov, L. S. Sunderlin, and P. B. Armentrout, *J. Chem. Phys.* **93**, 2676 (1990).
- ² E. Murad, *J. Geophys. Res.* **83**, 5525 (1978); E. Murad, Air Force Geophysics Laboratory, Hanscom Air Force Base, MA, Technical Report AFGL-TR-77-0235, 1977.
- ³ N. Aristov and P. B. Armentrout, *J. Am. Chem. Soc.* **106**, 4065 (1984).
- ⁴ N. Aristov and P. B. Armentrout, *J. Phys. Chem.* **90**, 5135 (1986).
- ⁵ D. Smith and N. G. Adams, *Plasma Chemistry I*, Vol. 89 of *Topics in Current Chemistry* (Springer-Verlag, Berlin, 1980), p. 1.
- ⁶ N. Aristov and P. B. Armentrout, *J. Am. Chem. Soc.* **108**, 1806 (1986).
- ⁷ M. W. Chase, C. A. Davies, J. R. Downey, D. J. Frurip, R. A. McDonald, and A. N. Syverud, *J. Phys. Chem. Ref. Data* **14**, Suppl. 1 (1985) (JANAF tables).
- ⁸ K. M. Ervin and P. B. Armentrout, *J. Chem. Phys.* **83**, 166 (1985).
- ⁹ P. J. Chantry, *J. Chem. Phys.* **55**, 2746 (1971).
- ¹⁰ L. S. Sunderlin and P. B. Armentrout, *J. Phys. Chem.* **92**, 1209 (1988).
- ¹¹ J. Sugar and C. Corliss, *J. Phys. Chem. Ref. Data* **14**, Suppl. 2 (1985).
- ¹² D. E. Clemmer, L. S. Sunderlin, and P. B. Armentrout, *J. Phys. Chem.* **94**, 208 (1990).
- ¹³ D. E. Clemmer, L. S. Sunderlin, and P. B. Armentrout, *J. Phys. Chem.* **94**, 3008 (1990).
- ¹⁴ N. Aristov and P. B. Armentrout, *J. Am. Chem. Soc.* **108**, 1806 (1986).
- ¹⁵ W. J. Chesnavich and M. T. Bowers, *J. Phys. Chem.* **83**, 900 (1979).
- ¹⁶ L. S. Sunderlin, N. Aristov, and P. B. Armentrout, *J. Am. Chem. Soc.* **109**, 78 (1987).
- ¹⁷ P. B. Armentrout and J. L. Beauchamp, *J. Chem. Phys.* **74**, 2819 (1981); *J. Am. Chem. Soc.* **103**, 784 (1981).
- ¹⁸ B. H. Boo and P. B. Armentrout, *J. Am. Chem. Soc.* **109**, 3549 (1987).
- ¹⁹ N. Aristov and P. B. Armentrout, *J. Phys. Chem.* **91**, 6178 (1987).
- ²⁰ P. B. Armentrout, *Annu. Rev. Phys. Chem.* **41**, 313 (1990); *Science* **251**, 175 (1991).
- ²¹ M. E. Weber, J. L. Elkind, and P. B. Armentrout, *J. Chem. Phys.* **84**, 1521 (1986).
- ²² B. H. Boo and P. B. Armentrout, *J. Am. Chem. Soc.* **109**, 3349 (1987); K. M. Ervin and P. B. Armentrout, *J. Chem. Phys.* **84**, 6738 (1986); **86**, 2659 (1987).
- ²³ P. B. Armentrout, in *Advances in Gas Phase Ion Chemistry*, edited by N. G. Adams and L. M. Babcock (JAI, Greenwich, CT, in press).
- ²⁴ D. E. Clemmer, N. Aristov, and P. B. Armentrout (unpublished).
- ²⁵ D. E. Clemmer, M. Knowles, N. Aristov, and P. B. Armentrout (unpublished).
- ²⁶ To convert $D_{298}^0(\text{MO}^+)$ to 0 K values, we require the 0 and 298 K enthalpies for Sc⁺, O, and ScO⁺. The values for the first two species are well known, but not those for ScO⁺. The change in enthalpy is known, however, for ScO, such that we assume here that the change in $D^0(\text{ScO}^+)$ from 298 to 0 K, $\Delta D^0(\text{ScO}^+)$, is nearly the same as that of $D^0(\text{ScO})$, $\Delta D^0(\text{ScO}) = 0.05$ eV (see Ref. 27). Any deviation from this value is accounted for by including an uncertainty of ± 0.02 eV.
- ²⁷ J. B. Pedley and E. M. Marshall, *J. Phys. Chem. Ref. Data* **12**, 967 (1983).
- ²⁸ R. Haque and K. A. Gingerich, *J. Chem. Phys.* **74**, 6407 (1981).
- ²⁹ G. H. Jeung and J. Koutecky, *J. Chem. Phys.* **88**, 3747 (1988).
- ³⁰ J. L. Tilson and J. F. Harrison, *J. Phys. Chem.* **95**, 5097 (1991).
- ³¹ E. A. Carter and W. A. Goddard III, *J. Phys. Chem.* **92**, 2109 (1988).
- ³² J. F. Harrison, *J. Phys. Chem.* **90**, 3313 (1986).
- ³³ P. B. Jasien and W. J. Stevens, *Chem. Rev. Lett.* **147**, 72 (1988).
- ³⁴ J. L. Elkind, L. S. Sunderlin, and P. B. Armentrout, *J. Phys. Chem.* **93**, 3151 (1989).
- ³⁵ J. L. Elkind and P. B. Armentrout, *Int. J. Mass Spectrom. Ion Processes* **83**, 259 (1988).
- ³⁶ J. L. Elkind and P. B. Armentrout, *J. Phys. Chem.* **89**, 5626 (1985).
- ³⁷ C. W. Bauschlicher and L. A. Barnes, *Chem. Phys.* **124**, 383 (1988).
- ³⁸ A. Mavridis, J. F. Harrison, and J. Allison, *J. Am. Chem. Soc.* **111**, 2482 (1989).
- ³⁹ The onset of product dissociation, process (5), begins exactly at $D^0(\text{CO}) = 11.11$ eV for all cases where the reactant and product Sc⁺ are in the same state and C and O are both in their ³P ground states. If the reactant Sc⁺ is in an excited state, the onset of process (5) will shift to lower energy, while if any of the products are in excited states, the onset of process (5) shifts to higher energies. Reaction of Sc⁺ (¹D) should shift the dissociation onset to lower energies by 0.3 eV, but the triplet states of ScO⁺ are calculated to dissociate to excited states of Sc⁺ (predominantly the ³F state at 0.6 eV). Thus, the shifts may cancel leading to an onset for dissociation within 0.3 eV of $D^0(\text{CO})$.
- ⁴⁰ J. L. Elkind and P. B. Armentrout, *J. Chem. Phys.* **84**, 4862 (1986).
- ⁴¹ For reactions (3) and (4), the true center-of-mass energy is $E_{\text{CM}} = \mu v^2/2$ where $\mu = m_{\text{Sc}}(m_{\text{C}} + m_{\text{O}})/M$, $M = m_{\text{Sc}} + m_{\text{C}} + m_{\text{O}}$, and v is the magnitude of the relative velocity of the reactants, $|v(\text{Sc}^+) - v(\text{CO})|$. This is the energy scale of Figs. 1–3. If, however, the interaction is an impulsive collision between Sc and C, or Sc and O, then the effective energy is $E_{\text{P}} = \mu' v^2/2$ where for reaction (3), $\mu' = m_{\text{Sc}} m_{\text{C}}/m_{\text{ScC}}$, and for reaction (4), $\mu' = m_{\text{Sc}} m_{\text{O}}/m_{\text{ScO}}$, and v is the same since $v_{\text{C}} = v_{\text{O}} = v_{\text{CO}}$. Then the effective energy on the pairwise energy scale is $E_{\text{P}} = E_{\text{CM}}(M m_{\text{C}}/m_{\text{ScC}} m_{\text{CO}}) = 0.55 E_{\text{CM}}$ for reaction (3) and $E_{\text{P}} = E_{\text{CM}}(M m_{\text{O}}/m_{\text{ScO}} m_{\text{CO}}) = 0.68 E_{\text{CM}}$ for reaction (4).
- ⁴² K. M. Ervin, J. L. Elkind, S. K. Loh, and P. B. Armentrout (unpublished).
- ⁴³ J. L. Elkind and P. B. Armentrout, *J. Phys. Chem.* **90**, 5736 (1986).